Journal of Sound and Vibration (2002) **258**(1), 45–63
doi:10.1006/jsvi.5071, available online at http://www.idealibrary.com on IDEAL®

EFFECTS OF MODE LOCALIZATION ON INPUT–OUTPUT DIRECTIONAL PROPERTIES OF STRUCTURES

A. MUĞAN

Mechanical Engineering Department, Istanbul Technical University, Gumuşsuyu 80191, *Istanbul, Turkey.* E-mail: mugan@itu.edu.tr

(*Received* 15 *May* 2000, *and in final form* 17 *December* 2001)

The singular-value decomposition (SVD) is employed to study the effects of localization phenomena on input–output relationships, and power and energy transmission ratios of structures. For weakly and strongly coupled systems, existence of strong localization of singular vectors and abrupt veering of singular value loci are shown. Occurrence of strong localization causes abrupt changes in input–output directional properties. In contrast to eigenvalues, singular values do not veer away by introducing a disorder in weakly coupled systems. In particular, the use of singular values and vectors is computationally advantageous in considering multiple load cases. While eigenvalue-based analyses give information about the resonance frequencies and vibration modes of a structure, singular values of the structure are related to the forced response characteristics and give the dynamic behavior in the frequency domain. Representative examples in structural dynamics are presented.

1. INTRODUCTION

It has long been known that inhibition of vibration propagation and localization of vibration modes may occur in weakly coupled structures due to the existence of small disorders. The vibration modes may change significantly to become strongly localized, showing extreme sensitivity against some parameters, if a small disorder is introduced to systems having weak internal coupling. This phenomenon is studied in various fields from the physics [1–5] to structural dynamics [6–14]. Leissa [15] showed that there exists an eigenvalue veering phenomenon corresponding to mode localization such that when two eigenvalue loci approach each other, they do not intersect and veer away from each other. By using a perturbation approach, Perkins and Mote [16] showed that eigenvalue veering may also occur in continuous systems. Pierre [11] proved that when a small disorder is introduced in conservative nearly periodic structures with weak internal coupling, both strong mode localization and veering of the eigenvalue loci occur that indicates these are two manifestations of the same phenomenon.

Consequences of both eigenvalue loci veering and mode localization phenomena are catastrophic since small changes in system parameters result in large variations in the eigenvalues and mode shapes respectively. Investigations into the effects of the disorder on vibration mode localization typically employ eigensolution analysis and, up to date, no attention has been paid to the behavior of singular values and vectors of systems. As developed in this paper, the singular-value decomposition (SVD)-based analysis is computationally advantageous in multiple load cases and well suited to study input–output relationships and power and energy transmission ratios of systems.

In this paper, input–output relationships of two representative systems are studied as follows: a mistuned nearly periodic assembly of coupled oscillators and a strongly coupled oscillator system. Existence of localization of singular-vectors and abrupt veering away of the singular value loci are shown at weakly and strongly coupled systems. Occurrence of localization causes abrupt changes in input–output relationships of a system that are closely related to the singular values and vectors of the system. The relationships between the singular values and power and energy transmission ratios are presented as well.

If forced vibrations of a structure in the existence of multiple load cases is studied, it is of engineering value to know the worst possible load case of the structure for which structural response for each load case should be investigated that is cumbersome. Since the singular vectors associated with the first singular value give the worst possible load case and corresponding structural response, it is particularly advantageous to use the SVD in multiple load cases due to reduced computational costs. Besides, while eigenvalue based analyses give information about the resonance frequencies and vibration modes of a structure, singular values of the structure are related to the forced response characteristics and give the dynamic behavior in the frequency domain. These are the main advantages of the proposed analysis technique based on the SVD presented in this paper. Some of the important results on the SVD are reviewed in the paper as well.

The outline of the article is as follows: we begin in section 2 by revisiting the properties of the SVD. In section 3, directional properties of the SVD are presented. The relationships among the singular vectors, singular values and corresponding matrix transfer function are derived in section 4. Applications of the SVD to representative examples are given in section 5, and conclusions are drawn in section 6.

2. PROPERTIES OF THE SINGULAR VALUE DECOMPOSITION

Based on the material in references [17] and [18], some properties of the SVD are revisited in this section. Consider the matrix $\mathbf{A} \in C^{m\times n}$, then there exist unitary matrices $\mathbf{U} \in C^{m\times m}$, $\mathbf{\Sigma} \in R^{m\times n}$ and $\mathbf{V} \in C^{n\times n}$ called the SVD of $\mathbf{A}$ such that $\mathbf{A}$ can be factored uniquely as

$$\mathbf{A} = \mathbf{U\Sigma V}^{\mathrm{H}}, \tag{1}$$

where the columns of $\mathbf{U} = [\mathbf{u}_1|\mathbf{u}_2|\cdots|\mathbf{u}_m]$ and $\mathbf{V} = [\mathbf{v}_1|\mathbf{v}_2|\cdots|\mathbf{v}_n]$ are, respectively, the left and right singular vectors, and $\mathbf{V}^{\mathrm{H}}$ is the conjugate transpose of $\mathbf{V}$. If $m = n$, which is the case for the systems in this paper, $\mathbf{\Sigma} = \mathrm{Diag}\{\sigma_1, \sigma_2, \ldots, \sigma_m\}$ where σ_i are the singular values of $\mathbf{A}$. Note that $\mathbf{u}_i$ and $\mathbf{v}_i$ are, respectively, orthonormal eigenvectors of $\mathbf{AA}^{\mathrm{H}}$ and $\mathbf{A}^{\mathrm{H}}\mathbf{A}$ such that

$$\mathbf{UU}^{\mathrm{H}} = \mathbf{I} \quad \text{and} \quad \mathbf{AA}^{\mathrm{H}}\mathbf{U} = \mathbf{U\Sigma}^2, \tag{2}$$

$$\mathbf{VV}^{\mathrm{H}} = \mathbf{I} \quad \text{and} \quad \mathbf{A}^{\mathrm{H}}\mathbf{AV} = \mathbf{V\Sigma}^2, \tag{3}$$

where $\mathbf{I}$ is the identity matrix. In addition, for a square matrix $\mathbf{A}$ having the following SVD if

$$\mathbf{A} = \mathbf{U\Sigma V}^{\mathrm{H}}, \quad \mathbf{A}^{-1} = \mathbf{V\Sigma}^{-1}\mathbf{U}^{\mathrm{H}}. \tag{4}$$

Although the singular values of $\mathbf{A}$ are uniquely defined, the singular vectors are not. If $\mathbf{A} = \mathbf{U\Sigma V}^{\mathrm{H}}$, then $\mathbf{A} = \mathbf{U}'\mathbf{\Sigma V}'^{\mathrm{H}}$ where $\mathbf{U}' = \mathbf{U}\mathrm{e}^{j\theta}$ and $\mathbf{V}' = \mathbf{V}\mathrm{exp}^{j\theta}$, where j is the imaginary unit, for any θ is also a SVD of $\mathbf{A}$.

3. DIRECTIONAL PROPERTIES

Consider the following time-independent linear equation system:

$$\mathbf{Kd} = \mathbf{f}, \tag{5}$$

where, in general, $\mathbf{K} \in \mathscr{C}^{n\times n}$, $\mathbf{d} \in \mathscr{C}^n$ and $\mathbf{f} \in \mathscr{C}^n$. Then, $\mathbf{d} = \mathbf{K}^{-1}\mathbf{f}$. Suppose that $\mathbf{K}^{-1}$ has the SVD of $\mathbf{K}^{-1} = \mathbf{U\Sigma V}^{\mathrm{H}}$, where $\mathbf{U} \in \mathscr{C}^{n\times n}$, $\mathbf{\Sigma} \in \mathscr{R}^{n\times n}$ and $\mathbf{V} \in \mathscr{C}^{n\times n}$. In order to show that the system has different gains for different input directions, the SVD of $\mathbf{K}^{-1}$ is written in the following dyadic form:

$$\mathbf{K}^{-1} = \sum_{i=1}^{n} \sigma_i \mathbf{u}_i \mathbf{v}_i^{\mathrm{H}}. \tag{6}$$

Beforehand assume that the singular values are distinct which is the case for physical systems considered here. If the force vector $\mathbf{f}$ is in the direction of the kth right singular vector $\mathbf{f} = \mathbf{v}_k$, then one has

$$\mathbf{d} = \sum_{i=1}^{n} \sigma_i \mathbf{u}_i \mathbf{v}_i^{\mathrm{H}} \mathbf{v}_k. \tag{7}$$

Since $\mathbf{v}_i$ are orthonormal, $\mathbf{v}_i^{\mathrm{H}}\mathbf{v}_k = \delta_{ik}$ where δ_{ik} is the Kronecker delta function, we get

$$\mathbf{d} = \sigma_k \mathbf{u}_k \tag{8}$$

and

$$||\mathbf{d}||_2 = \sigma_k. \tag{9}$$

Note that equation (8) shows that if $\mathbf{f}$ is in the direction of $\mathbf{v}_k$, the output $\mathbf{d}$ is in the direction of $\mathbf{u}_k$, and equation (9) shows that the system's gain is equal to σ_k. In brief, each right singular vector tells us how we would place an input into the system to produce a gain equal to the associated singular value, and the corresponding left singular vector tells us how the response to this input is distributed among the different degrees of freedom [19].

For the application of the SVD to semidiscrete equation systems, consider the following matrix equation of structural dynamics

$$\mathbf{M\ddot{d}} + \mathbf{C\dot{d}} + \mathbf{Kd} = \mathbf{f}, \tag{10}$$

where $\mathbf{M} \in \mathscr{R}^{n\times n}$ is the mass matrix, $\mathbf{C} \in \mathscr{R}^{n\times n}$ the viscous damping matrix, $\mathbf{K} \in \mathscr{R}^{n\times n}$ the stiffness matrix, $\mathbf{f} \in \mathscr{R}^n$ the vector of applied forces, and $\mathbf{d} \in \mathscr{R}^n$, $\dot{\mathbf{d}}$ and $\ddot{\mathbf{d}}$ are, respectively, the displacement, velocity and acceleration vectors. By taking the Laplace transform of equation (10), one get

$$\mathbf{D}(s) = \mathbf{G}(s)\mathbf{F}(s), \tag{11}$$

where the matrix transfer function $\mathbf{G}(s)$ is defined by

$$\mathbf{G}(s) = (\mathbf{M}s^2 + \mathbf{C}s + \mathbf{K})^{-1}. \tag{12}$$

Then, the steady state output $\mathbf{D}(\mathrm{j}\omega)$ of this system in response to the sinusoidal input of frequency ω, i.e., $\mathbf{f}(t) = \tilde{\mathbf{f}}\sin(\omega t)$, is given by

$$\mathbf{D}(\mathrm{j}\omega) = \mathbf{G}(\mathrm{j}\omega)\tilde{\mathbf{f}}, \tag{13}$$

where $\tilde{\mathbf{f}}$ is the input magnitude vector. In equation (13), the magnitude of $D_i(\mathrm{j}\omega)$ is the magnitude of the ith component of the output vector $\mathbf{d}$, while the phase of $D_i(\mathrm{j}\omega)$ is the phase angle between the ith component of the output vector $\mathbf{d}$ and the input $\mathbf{f}$. Similar to the time-independent case, if $\tilde{\mathbf{f}}$ is in the direction of $\mathbf{v}_k$, the response $\mathbf{D}(\mathrm{j}\omega)$ will be in the direction of $\mathbf{u}_k$ having the gain of σ_k. Note that the singular values and vectors are to be the function of the excitation frequency ω, and we adopt the ordering $\sigma_1 \geqslant \sigma_2 \geqslant \cdots \geqslant \sigma_n \geqslant 0$.

4. INPUT–OUTPUT RELATIONSHIPS

Suppose that the system is represented in terms of the Laplace transformed variables as in equation (11). For a sinusoidal excitation of frequency ω, by neglecting the argument $s = \mathrm{j}\omega$, the SVD of $\mathbf{G}$ is given by $\mathbf{G} = \mathbf{U\Sigma V}^{\mathrm{H}}$. Since $\{\mathbf{v}_i\}$ form a basis, an input in any direction can be represented by

$$\mathbf{F} = \sum_{i=1}^{n} a_i \mathbf{v}_i. \tag{14}$$

The coefficients a_i can be computed via the orthonormal property of $\mathbf{v}_i$ as follows:

$$a_i = \langle \bar{\mathbf{v}}_i, \mathbf{F} \rangle, \tag{15}$$

where $\langle \cdot, \cdot \rangle$ defines the L_2 inner product and a superposed bar denotes conjugation. Then, the output $\mathbf{D}$ can be computed by

$$\mathbf{D} = \left(\sum_{i=1}^{n} \sigma_i \mathbf{u}_i \mathbf{v}_i^{\mathrm{H}} \right) \quad \mathbf{F} = \sum_{i=1}^{n} a_i \sigma_i \mathbf{u}_i \tag{16}$$

and the transfer function between the ith output and the jth input is given by

$$G_{ij} = \frac{\partial D_i}{\partial F_j} = \sum_{m=1}^{n} \sigma_m u_{m,i} \bar{v}_{m,j}, \tag{17}$$

where D_i is the ith entry of $\mathbf{D}$, $u_{m,i}$ is the ith entry of $\mathbf{u}_m$ and σ_m is the mth singular value of $\mathbf{G}(s)$ and so on. Note that the input–output sensitivities, i.e., G_{ij} terms, increase as σ_1 increases, in other words, as $(\mathbf{M}s^2 + \mathbf{C}s + \mathbf{K})$ gets close to the singularity which may occur for a complex frequency $s = \mathrm{j}\omega$ while it may not for other frequencies. The contribution of the first singular value σ_1 and associated singular vectors in equation (17) is dominant since σ_1 is the largest singular value.

4.1. ANALYSIS OF CURVE VEERING AND LOCALIZATION

It is shown in reference [11] that even though classical perturbation methods fail to describe localization phenomenon of weakly coupled systems, they provide useful insight into the onset of localization. In order to handle the dramatic changes resulting from small disorders, a modified perturbation method is developed in references [12, 13] where the small coupling between component systems which governs the small distance between eigenvalues is treated as a perturbation while the parameter irregularities are included in the unperturbed system. On the other hand, while the modified perturbation method detects the change in the direction of the loci, it fails for the disorders of order ε^2 or smaller degree, namely, the eigenvalue loci veering region, in which case one must use a classical procedure [11].

Recall that $\mathbf{U}$, $\mathbf{\Sigma}$ and $\mathbf{V}$ are defined by the eigensolution problems in equations (2) and (3) as follows: $\mathbf{u}_i$ the eigenvectors in equations (2), $\mathbf{v}_i$ the eigenvectors in equations (3) and $\boldsymbol{\sigma}_i^2$ the eigenvalues in both equations (2) and (3). It is straightforward to compute the perturbations in the SVD of a matrix by using the results of the perturbations of eigensolutions; hence, the analyses based upon perturbation methods in references [11–13] can also be applied to singular vectors and squares of the singular values to detect the onset of localization. Similarly, the sensitivity analysis results about the eigensolutions in the literature are applicable to perturbations in σ_i^2, $\mathbf{u}_i$ and $\mathbf{v}_i$ as well.

Lemma. *Consider the following parameterized system*

$$(\mathbf{K} + \varepsilon\mathbf{A})\mathbf{d}(\varepsilon) = \mathbf{f} + \varepsilon\mathbf{b} \tag{18}$$

whose solution $\mathbf{x}(\varepsilon)$ *has the following form*:

$$\mathbf{x}(\varepsilon) = \mathbf{x} + \varepsilon\dot{\mathbf{x}}(0) + O(\varepsilon^2), \tag{19}$$

where $\dot{\mathbf{x}}(0) = \mathbf{K}^{-1}(\mathbf{b} - \mathbf{A}\mathbf{x})$. *Then, the following holds for any vector norm and consistent matrix norm*

$$\frac{||\mathbf{x}(\varepsilon) - \mathbf{x}||}{||\mathbf{x}||} \leqslant \varepsilon||\mathbf{K}^{-1}||\left(\frac{||\mathbf{b}||}{||\mathbf{x}||} + ||\mathbf{A}||\right) + O(\varepsilon^2). \tag{20}$$

Proof. See page 79 of reference. [20].

If the matrix transfer function $\mathbf{G}(s) = (\mathbf{M}s^2 + \mathbf{C}s + \mathbf{K})^{-1}$ has the SVD of $\mathbf{G} = \sum_{i=1}^{n} \sigma_i \mathbf{u}_i \mathbf{v}_i^{\mathrm{H}}$ for a complex frequency $s = \mathrm{j}\omega$, then following equation (20) it is concluded that $O(\varepsilon)$ perturbations in $\mathbf{M}$, $\mathbf{C}$, $\mathbf{K}$ and force vector $\mathbf{f}$ result in changes in the solutions by an amount of $\varepsilon\sigma_1$, where σ_1 is the largest singular value of $(\mathbf{M}s^2 + \mathbf{C}s + \mathbf{K})^{-1}$.

4.2. ENERGY DISSIPATION AND SINGULAR VALUES

It is shown in references [21,22] that singular values give a frequency-domain characterization for the limits to some appropriately defined gains. For a deterministic periodic input signal $\mathbf{f}$ of frequency ω, sum of the mean-squared values of the steady state outputs $\mathbf{d}_{ss}$ over one period is given by

$$SMSVO(\omega) = \frac{\omega}{2\pi}\int_0^{2\pi/\omega} \mathbf{d}_{ss}^{\mathrm{T}}(t)\,\mathbf{d}_{ss}(t)\,\mathrm{d}t = \frac{1}{2}\mathbf{f}^{\mathrm{T}}\mathbf{S}(\omega)\mathbf{f}, \tag{21}$$

where

$$\mathbf{S}(\omega) = \tfrac{1}{2}[\mathbf{G}^{\mathrm{H}}(\mathrm{j}\omega)\mathbf{G}(\mathrm{j}\omega) + \overline{\mathbf{G}^{\mathrm{H}}(\mathrm{j}\omega)\mathbf{G}(\mathrm{j}\omega)}] \tag{22}$$

On the other hand, sum of the mean-squared values of the inputs over one period is

$$SMSVI = \frac{\omega}{2\pi}\int_0^{2\pi/\omega} \mathbf{f}^{\mathrm{T}}(t)\mathbf{f}(t)\,\mathrm{d}t = \frac{1}{2}\mathbf{f}^{\mathrm{T}}\mathbf{f}. \tag{23}$$

Then,

$$\sigma_1^2(\omega) \geqslant \frac{SMSVO(\omega)}{SMSVI} \geqslant \sigma_n^2(\omega). \tag{24}$$

For a deterministic aperiodic input, equation (24) becomes

$$\sigma_1^2(\omega) \geqslant \frac{||\hat{\mathbf{d}}(\mathrm{j}\omega)||_2^2}{||\hat{\mathbf{f}}(\mathrm{j}\omega)||_2^2} \geqslant \sigma_n^2(\omega). \tag{25}$$

where

$$\frac{||\hat{\mathbf{d}}(\mathrm{j}\omega)||_2^2}{||\hat{\mathbf{f}}(\mathrm{j}\omega)||_2^2} = \frac{\sum_{i=1}^{n} |\hat{d}_i(\mathrm{j}\omega)|^2}{\sum_{i=1}^{n} |\hat{f}_i(\mathrm{j}\omega)|^2} = \frac{\text{sum of energy densities of the outputs at } \omega}{\text{sum of energy densities of the inputs at } \omega} \tag{26}$$

and the superposed hat denotes the Fourier transformed variables as follows:

$$\hat{f}_i(\mathrm{j}\omega) = \int_{-\infty}^{\infty} f_i(t)\mathrm{e}^{-\mathrm{j}\omega t}\,\mathrm{d}t. \tag{27}$$

For a stochastic input signal, equation (24) becomes

$$\sigma_1^2(\omega) \geqslant \frac{trace[P_d(\omega)]}{trace[P_f(\omega)]} \geqslant \sigma_n^2(\omega), \tag{28}$$

where $P_d(\omega)$ and $P_f(\omega)$ are, respectively, the Fourier transforms of the covariance matrices of the output and input vector processes. For the proofs, see references [21,22]. Following equations (24) and (25), one can think of σ_1^2 and σ_n^2 as the limits to the average power transmission ratio for periodic input signals and the energy transmission ratio for aperiodic input signals. The upper bound is achieved if the input is placed in the direction of $\mathbf{v}_1$, and the lower bound is achieved if the input is placed in the direction of $\mathbf{v}_n$.

5. NUMERICAL EXAMPLES

In this section, input–output relationships of two representative systems are studied by using singular values and vectors as follows: a mistuned assembly of coupled oscillators and a strongly coupled oscillator system. All numerical simulations are completed by using the MATLAB.

5.1. A MISTUNED ASSEMBLY OF COUPLED OSCILLATORS

Consider the disordered system of two coupled oscillators shown in Figure 1. By using the SVD, forced response characteristics of the coupled oscillators are studied in this section. The governing equations of motion for small angles are as follows

$$m\ell^2\ddot{\theta}_1 = f_1\ell - k\ell^2\theta_1 - k(\ell\theta_1 - \ell(1+\Delta\ell)\theta_2)\ell - mg\ell\theta_1, \tag{29}$$

$$m\ell^2(1+\Delta\ell)^2\ddot{\theta}_2 = f_2\ell(1+\Delta\ell) + k(\ell\theta_1 - \ell(1+\Delta\ell)\theta_2)\ell(1+\Delta\ell) - mg\ell(1+\Delta\ell)\theta_2. \tag{30}$$

By taking the Laplace transform of both equations and arranging them, one gets

$$\left(\frac{\ell}{g}\right)s^2\theta_1(s) + (1+2R^2)\theta_1(s) - R^2(1+\Delta\ell)\theta_2(s) = \frac{F_1(s)}{mg}, \tag{31}$$

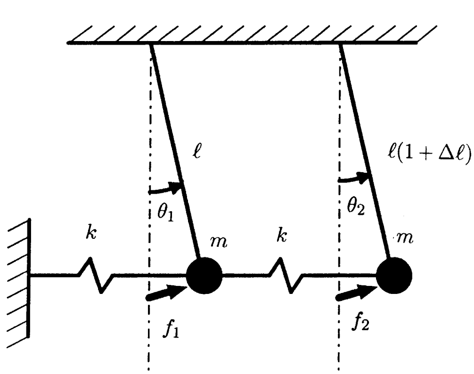

Figure 1. Two coupled oscillators.

$$\left(\frac{\ell}{g}\right)(1+\Delta\ell)s^2\theta_2(s)+\left(1+R^2(1+\Delta\ell)\right)\theta_2(s)-R^2\theta_1(s)=\frac{F_2(s)}{mg}. \quad (32)$$

By defining $\tilde{\theta_1}=\theta_1/(1+\Delta\ell)$ and $\tilde{\theta_2}=\theta_2$ to obtain symmetric system matrices, equations (31) and (32) can be cast into the following form

$$\tilde{\mathbf{\Theta}}(s)=\left(\mathbf{M}s^2+\mathbf{K}\right)^{-1}\mathbf{F}(s), \quad (33)$$

where **M** and **K** are symmetric, ℓ is the nominal length of the pendulums, $\Delta\ell$ the second pendulum's dimensionless length deviation from the nominal length, ω the excitation frequency, $\lambda=\omega^2/(g/\ell)$ the dimensionless eigenvalue, $R^2=(k/m)/(g/\ell)$ the dimensionless coupling, $\tilde{\mathbf{\Theta}}(s)=[\tilde{\theta_1}(s)\tilde{\theta_2}(s)]^{\mathrm{T}}$, and $\mathbf{F}(s)=[F_1(s)/(mg)F_2(s)/(mg)]^{\mathrm{T}}$. For $\Delta\ell=0$, the system is called tuned or ordered; otherwise, it is mistuned or disordered. Free vibration modes, mode localization and eigenvalue loci veering phenomena of this system are studied in references [11, 12], where in the existence of small disorder strong mode localization is reported for weakly coupled systems whereas mode shapes and eigenvalues of strongly coupled system do not manifest localization. Similar phenomena are observed in input–output relationships of this system as well.

Suppose that one is interested in the worst possible load case, which can be formulated as the solution of the following problem: find the displacement vector **d** in response to the worst loading **f**; that is,

Find

$$\max||\mathbf{d}||_2 \quad \text{s.t.} \quad ||\mathbf{f}||_2=1, \quad (34)$$

where the forcing vector length is set to unity $||\mathbf{f}||_2=1$ to quantify the input–output relationships uniquely. By definition of singular values in reference [23], the above problem defined by equation (34) is equivalent to finding the largest singular value σ_1 of the transfer function matrix **G** between the input **f** and the output **d** as follows: if σ_i is the ith singular value of the matrix **G**, then

$\sigma_1=\max\{||\mathbf{Gx}||_2:\ \mathbf{x}\in C^n,\ ||\mathbf{x}||_2=1\}$, so $\sigma_1=||\mathbf{Gw_1}||_2$ for some unit vector $\mathbf{w}_1\in C^n$,
$\sigma_2=\max\{||\mathbf{Gx}||_2:\ \mathbf{x}\in C^n,\ ||\mathbf{x}||_2=1,\ \mathbf{x}\perp\mathbf{w}_1\}$, so $\sigma_2=||\mathbf{Gw_2}||_2$ for some unit vector $\mathbf{w}_2\in C^n$ such that $\mathbf{w}_2\perp\mathbf{w}_1$,
...
$\sigma_k=\max\{||\mathbf{Gx}||_2:\ \mathbf{x}\in C^n,\ ||\mathbf{x}||_2=1,\ \mathbf{x}\perp\mathbf{w}_1,\dots,\mathbf{w}_{k-1}\}$, so $\sigma_k=||\mathbf{Gw_k}||_2$ for some unit vector $\mathbf{w}_k\in C^n$such that $\mathbf{w}_k\perp\mathbf{w}_1,\ \dots,\ \mathbf{w}_{k-1}$.

Instead of solving the original problem defined by equation (34), finding the largest singular value σ_1 is computationally cheaper, because it eliminates the need to find the worst possible load case which is cumbersome. As revisited in section 2, the right singular vector $\mathbf{v}_1$ and left singular vector $\mathbf{u}_1$ give the worst possible loading direction and the corresponding structural response respectively. Thus, the original problem reduces to finding the maximum eigenvalue of $\mathbf{GG}^{\mathrm{H}}$ which is computationally much cheaper to solve. For instance, in order to solve equation (34) for ten coupled pendulums with four external force terms, if a constrained optimization algorithm employing the Newton method in the International Mathematical Subroutines Library (IMSL) is used to compute the worst load case, it is found to be about 90 times slower than the SVD. If the problem size increases, the difference between the CPU times of the SVD-based analysis and conventional methods even deepens. Note that there is no need to compute all the singular values, because only the first singular value and associated singular vectors are needed that can be computed very efficiently by using selective algorithms, e.g., see references [18, 20].

The following parameter values are used in the numerical studies: $g = 10$, $\ell = 1$, $k = 1$, $m = 640$ for a weakly coupled system ($R = 0{\cdot}0125$) and $k = 1600$ for a strongly coupled system ($R = 0{\cdot}5$). For limited space, only the results of the first singular value σ_1 and associated left singular vector $\mathbf{u}_1$ are presented here. Since the system matrices $\mathbf{M}$ and $\mathbf{K}$ are symmetric in equation (33), right singular vectors $\mathbf{v}_i$ are equal to $\mathbf{u}_i$. Considering the SVD of the matrix transfer function $\mathbf{G}(s) = \left(\mathbf{M}s^2 + \mathbf{K}\right)^{-1}$ of the weakly coupled system, the singular value loci σ_1 is presented in Figure 2, and the components of the associated left singular vector $\mathbf{u}_1$ are given in Figures 3 and 4, where ω_{ri} are the natural frequencies and $u_{1,j}$ denotes the jth component of $\mathbf{u}_1$. Note that while $\mathbf{u}_1$ is the worst possible load case and the corresponding structural response ($\mathbf{u}_1 = \mathbf{v}_1$ in this problem), σ_1 is the corresponding structural power and energy transmission ratios. The peaks in singular-value loci correspond to resonance frequencies. These plots show the way the system will respond to a sinusoidal excitation of frequency ω at steady state. Since there is no damping in the system, components of the singular vectors exhibit jumps at resonance frequencies.

Contrary to the loci of eigenvalues in reference [11], the singular value loci of the weakly coupled oscillators in Figure 2 are almost insensitive to changes in the disorder $\Delta\ell$. As singular values of a system are the bounds of the system's energy and power transmission ratios due to equation (24), (25) and (28), it means that the system's power and energy transmissions are almost insensitive to changes in the disorder $\Delta\ell$ in all frequencies. The loci of both singular values of the weakly coupled system are shown in Figure 5 for $\Delta\ell = 0{\cdot}005$ in which one can observe the singular value veering phenomena about $\omega = 3{\cdot}158$ rad/s. As the amount of the disorder $\Delta\ell$ increases, the gap between the two peaks of σ_1 corresponding to resonance frequencies of the system increases having a curve veering in the middle of the peaks. Components of singular vectors change abruptly at resonance

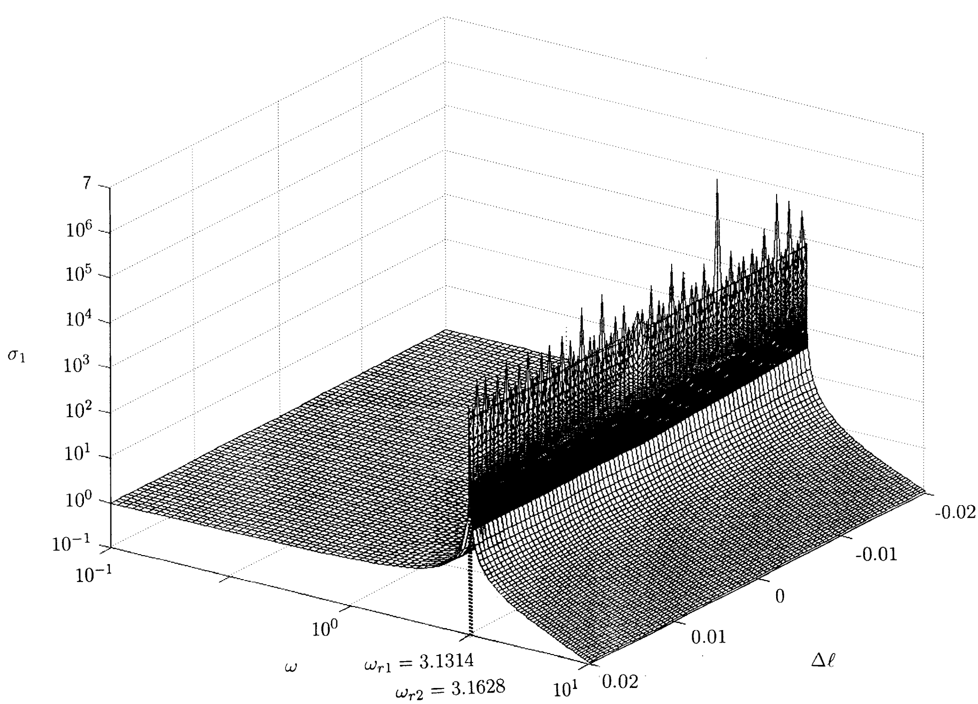

Figure 2. The singular value σ_1 where $R = 0{\cdot}0125$.

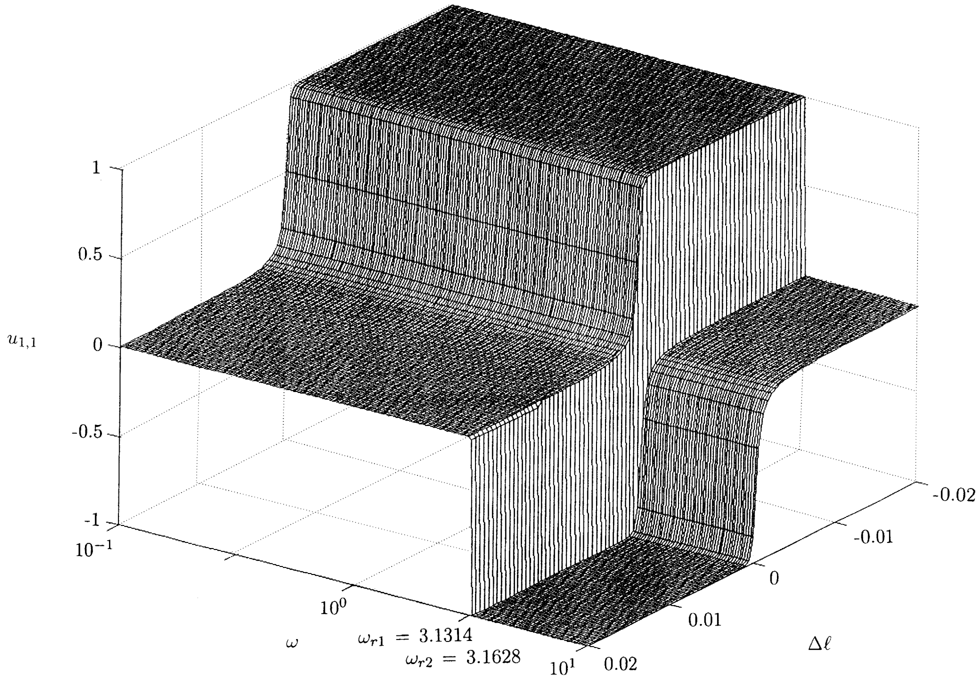

Figure 3. The left singular-vector component $u_{1,1}$ where $R = 0{\cdot}0125$.

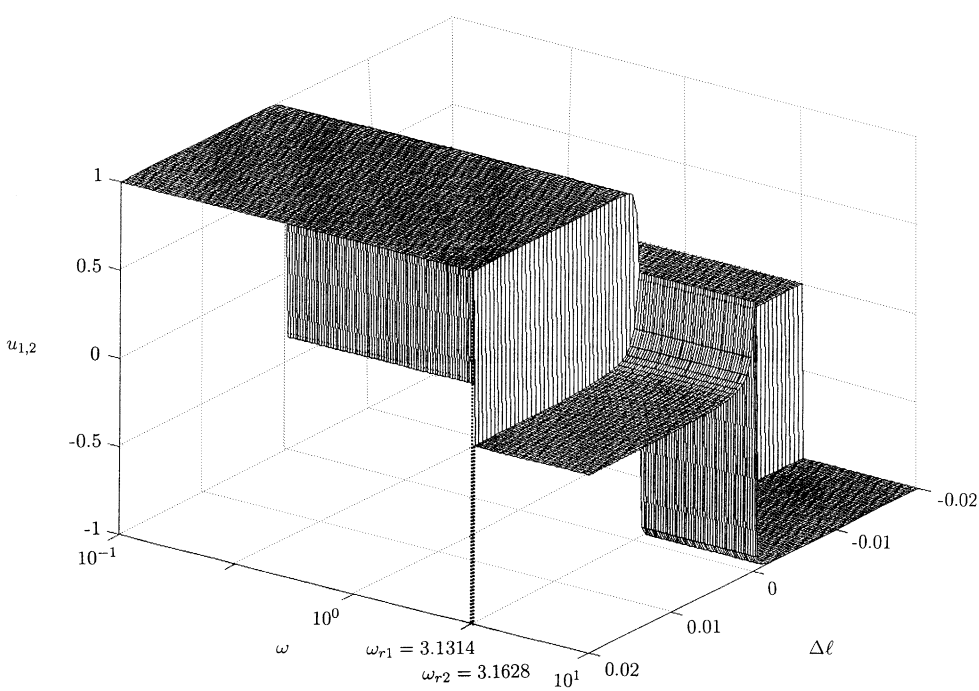

Figure 4. The left singular-vector component $u_{1,2}$ where $R = 0{\cdot}0125$.

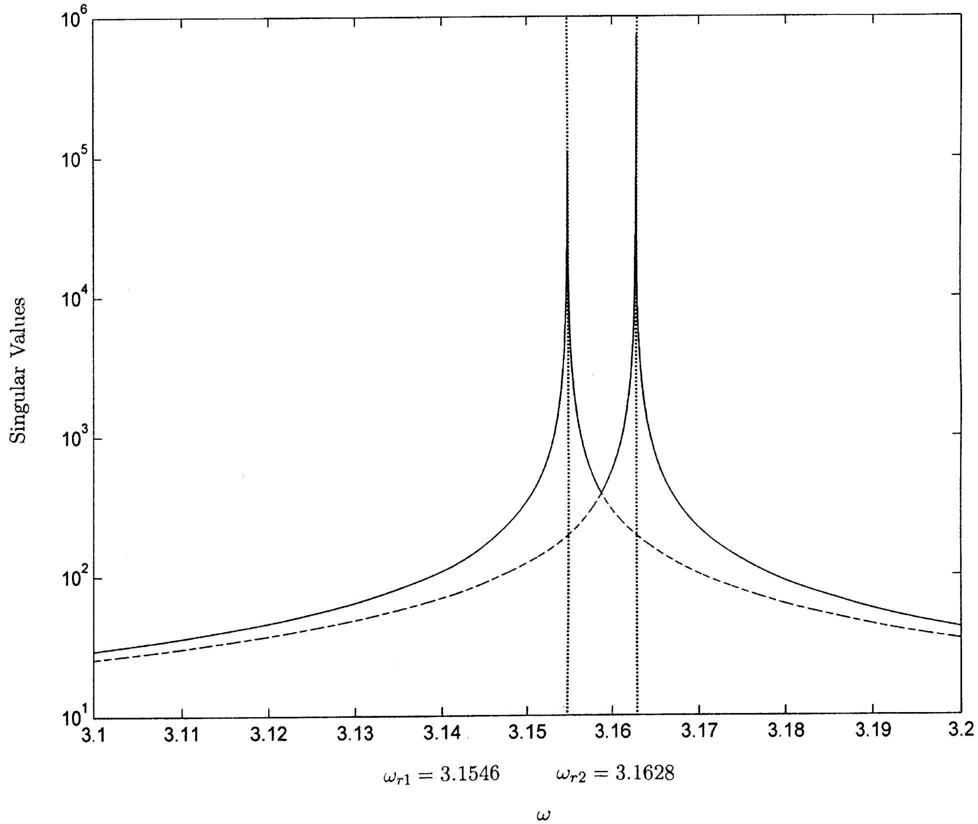

Figure 5. The singular-value veering phenomena for weakly coupled system for $R = 0{\cdot}0125$ and $\Delta\ell = 0{\cdot}005$. (—— σ_1; - - - - - - - σ_2).

frequencies, $\omega = 3{\cdot}158$ rad/s and $\Delta\ell = 0$ whereas the corresponding changes in singular values are smooth. This result means the power and energy transmission ratios are smooth; however, distribution of the total energy among different degrees of freedom may change abruptly as determined by the left singular vectors $\mathbf{u}_i$.

For the strongly coupled system, the singular-value plot σ_1 is presented in Figure 6, and components of the associated left singular vector $\mathbf{u}_1$ are given in Figures 7 and 8. For $\Delta\ell = 0{\cdot}005$, the singular value veering phenomena occurs about $\omega = 3{\cdot}71$ rad/s as shown in Figure 9. Components of singular vectors change abruptly at the peaks of σ_1 (i.e., resonances), $\omega = 3{\cdot}71$ rad/s and $\Delta\ell = 0$.

It is noteworthy that while eigenvalue-based analyses give the resonance frequencies and vibration modes of a structure, singular values are related to the forced response characteristics and give the system gain as a function of the excitation frequency. For both weakly and strongly coupled systems, it is concluded that the power and energy transmission ratios do not show abrupt changes due to the disorder because the singular values do not show abrupt changes due to the disorder. Hence, the power or energy of the system is not dissipated in the existence of strong mode localization but just concentrated at certain degrees-of-freedom which are determined by the singular vectors. While these power and energy transmission ratios may be large at certain excitation frequencies as a result of resonance, they may be small at some other excitation frequencies, e.g., see σ_i loci. The frequencies at which singular value veering phenomenon occurs have a special

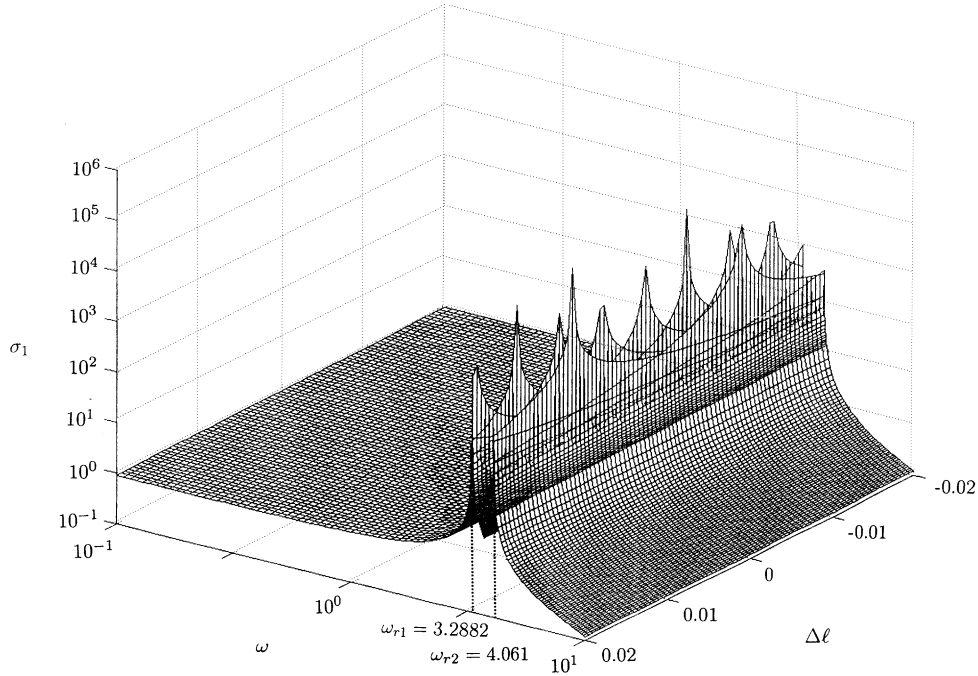

Figure 6. The singular value σ_1 where $R = 0{\cdot}5$.

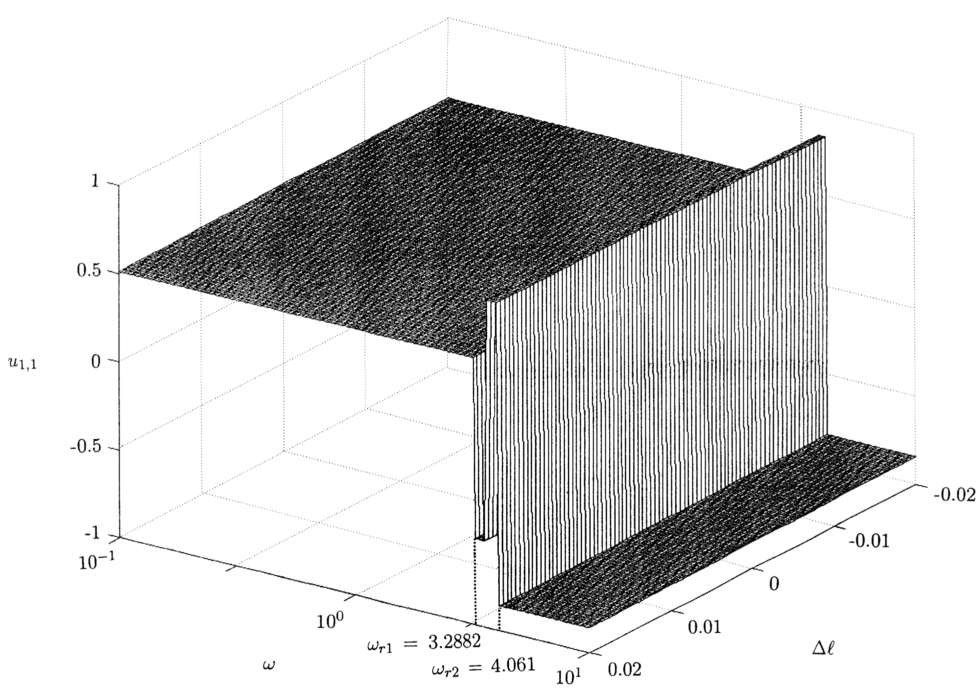

Figure 7. The left singular-vector component $u_{1,1}$ where $R = 0{\cdot}5$.

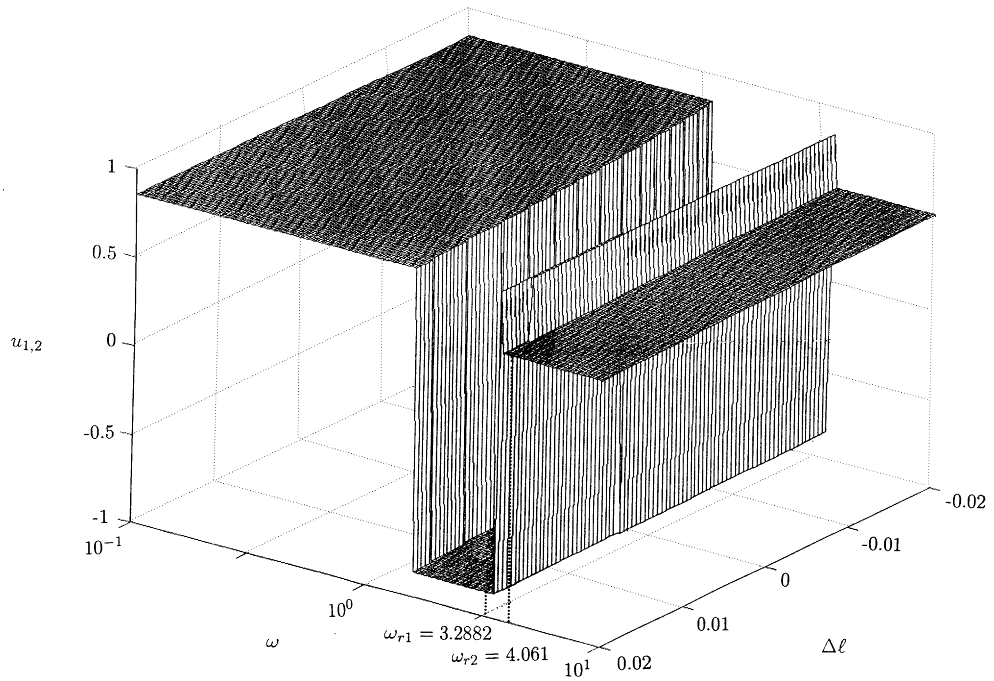

Figure 8. The left singular-vector component $u_{1,2}$ where $R = 0{\cdot}5$.

meaning as follows: two singular values are almost equal to each other at such frequencies whereas their singular vectors are completely different. It means that while the system has almost the same power and energy transmission ratios at these frequencies, forced response characteristics are quite different. Subsequently, these frequencies will be called *isopower frequencies*.

The difference between the maximum and minimum singular values $(\sigma_1 - \sigma_n)$ of the tuned system, i.e., $\Delta\ell = 0$, having $n = 2$ and 50 components are given in Figure 10. Observe that as the number of components in tuned systems increases, the bounds set by the singular values on power and energy transmission of the system (i.e., σ_1 and σ_n) change insignificantly; thus, the power and energy transmission ratios are almost insensitive to the number of oscillators for tuned systems. The bandwidth $(\sigma_1 - \sigma_n)$ is very tight, which is typical for nearly periodic tuned systems as well; consequently, there is not significant difference among the power and energy transmission ratios if the input is placed in the direction of different right singular vectors $\mathbf{v}_i$. For the tuned system, the power and energy transmission ratios are mainly affected by the excitation frequency ω, e.g., see Figure 10. In contrast, mistuned systems do not have tight $(\sigma_1 - \sigma_n)$ bandwidths and a small disorder in the system may result in significant changes in $(\sigma_1 - \sigma_n)$, e.g., see Figures 5 and 9.

5.2. A STRONGLY COUPLED OSCILLATOR SYSTEM

It is shown in this example that singular-value veering and singular-vector localization may arise naturally in strongly coupled systems as a function of the excitation frequency ω without any disorder. Consider the coupled mass–dashpot–spring system shown in

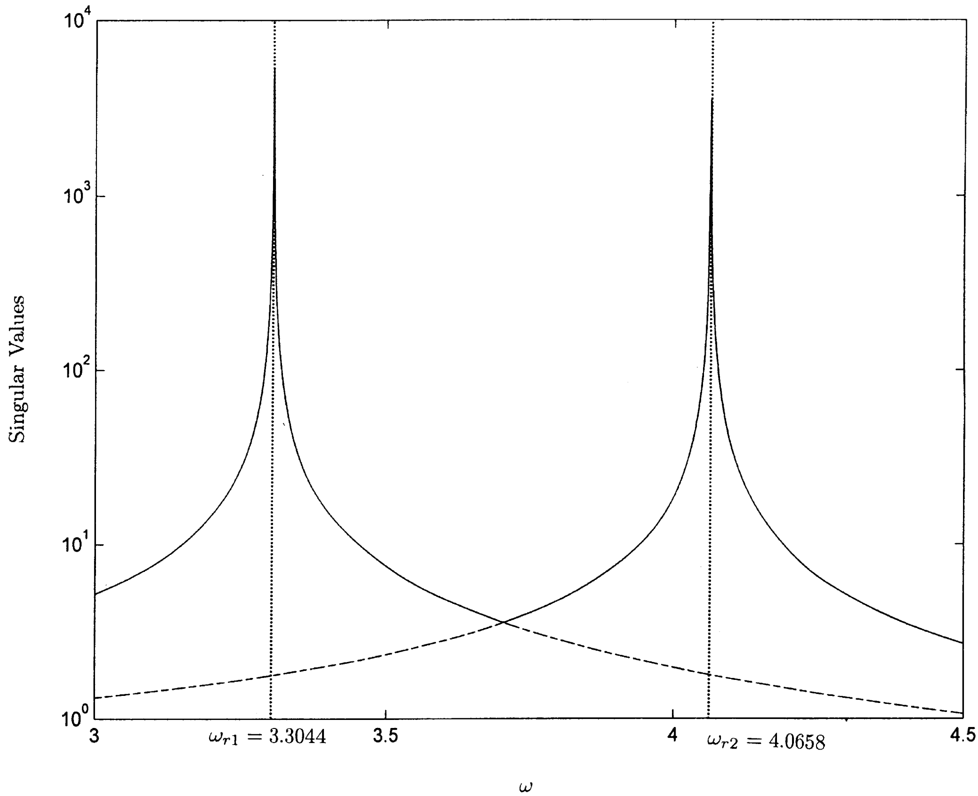

Figure 9. The singular-value veering phenomena for strongly coupled system for $R = 0{\cdot}5$ and $\Delta\ell = 0{\cdot}005$. (—— σ_1; - - - - - - σ_2).

Figure 11 whose parameters m_i, c_i and k_i are listed in Table 1. The equations of motion are as follows:

$$\mathbf{M}\ddot{\mathbf{d}} + \mathbf{C}\dot{\mathbf{d}} + \mathbf{K}\mathbf{d} = \mathbf{f}, \tag{35}$$

where

$$\mathbf{d} = [x_1 \;\; x_2 \;\; x_3]^{\mathrm{T}}, \tag{36}$$

$$\mathbf{f} = [f_1 \;\; f_2 \;\; f_3]^{\mathrm{T}}, \tag{37}$$

$$\mathbf{M} = \mathrm{Diag}\{m_1, m_2, m_3\} \tag{38}$$

$$\mathbf{C} = \begin{bmatrix} c_1 + c_2 & -c_2 & 0 \\ -c_2 & c_2 + c_3 & -c_3 \\ 0 & -c_3 & c_3 \end{bmatrix}, \tag{39}$$

$$\mathbf{K} = \begin{bmatrix} k_1 + k_2 & -k_2 & 0 \\ -k_2 & k_2 + k_3 & -k_3 \\ 0 & -k_3 & k_3 \end{bmatrix} \tag{40}$$

that represent a strongly coupled system. The corresponding matrix transfer function is defined by $\mathbf{G}(s) = (\mathbf{M}s^2 + \mathbf{C}s + \mathbf{K})^{-1}$ whose SVD is denoted by $\mathbf{G} = \mathbf{U}\boldsymbol{\Sigma}\mathbf{V}^{\mathrm{H}}$. The singular

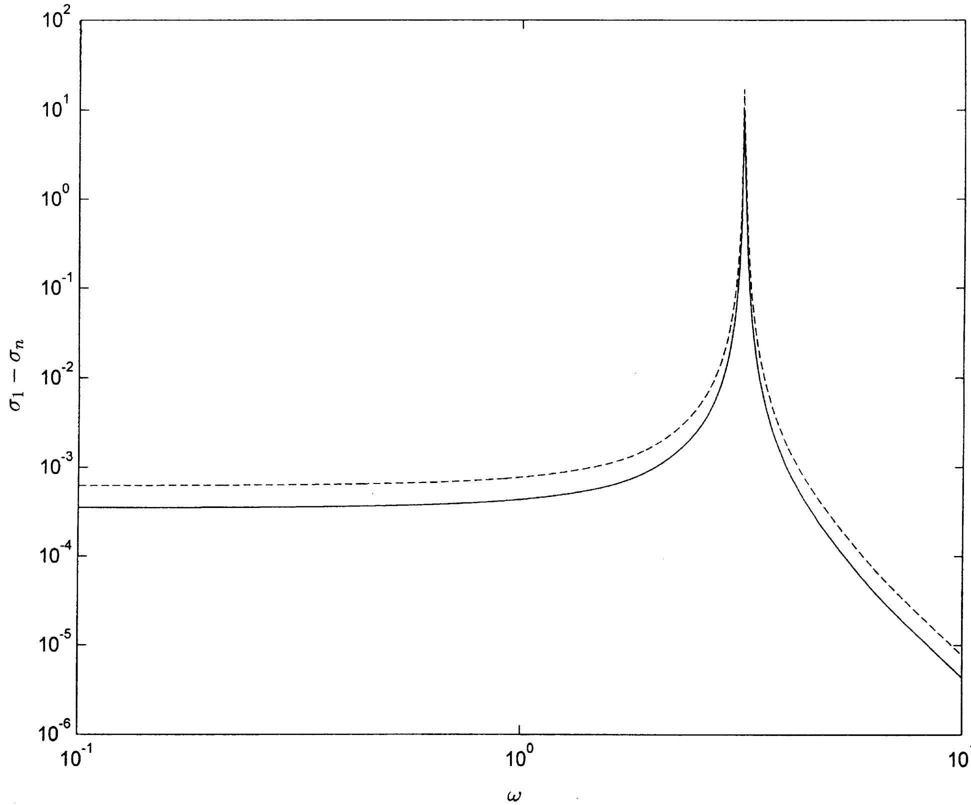

Figure 10. $\sigma_1 - \sigma_n$ for the tuned systems having $n = 2$ and 50 components. (—— $n = 2$; - - - - - - $n = 50$).

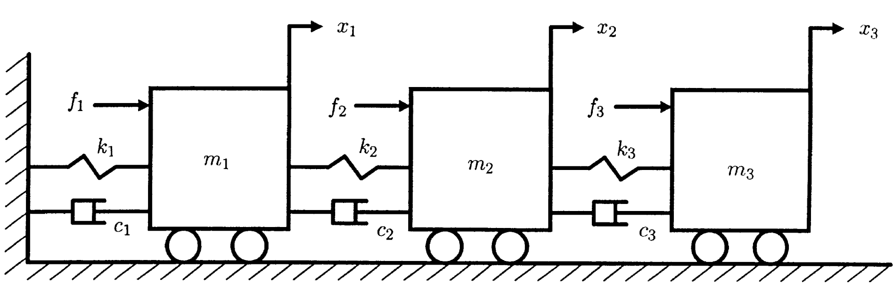

Figure 11. The mass–dashpot–spring system.

values σ_i and components of the left singular vectors $\mathbf{u}_i$ of $\mathbf{G}(s)$ are shown in Figures 12–15 as a function of the excitation frequency ω. Note that $\mathbf{v}_i = \mathbf{u}_i$ for this problem because $\mathbf{G}$ is symmetric, i.e., $\mathbf{GG}^{\mathrm{H}} = \mathbf{G}^{\mathrm{H}}\mathbf{G}$ in equations (2) and (3). The loci of σ_1 and σ_2 veer away at $\omega = 0{\cdot}1825$ and $\omega = 0{\cdot}6151$ rad/s, and the loci of σ_2 and σ_3 veer away at $\omega = 0{\cdot}3872$ rad/s (i.e., isopower frequencies). These loci cannot cross because there is no multiple singular value for the system, that results in a mutual repulsion of the loci, or curve veering. When the singular-values veer away, corresponding singular vectors show abrupt changes. For

TABLE 1

The parameters of mass–dashpot–spring system

Parameters	$i = 1$	$i = 2$	$i = 3$
m_i	100	20	25
c_i	1.2	0.2	0.8
k_i	0.3	3	7

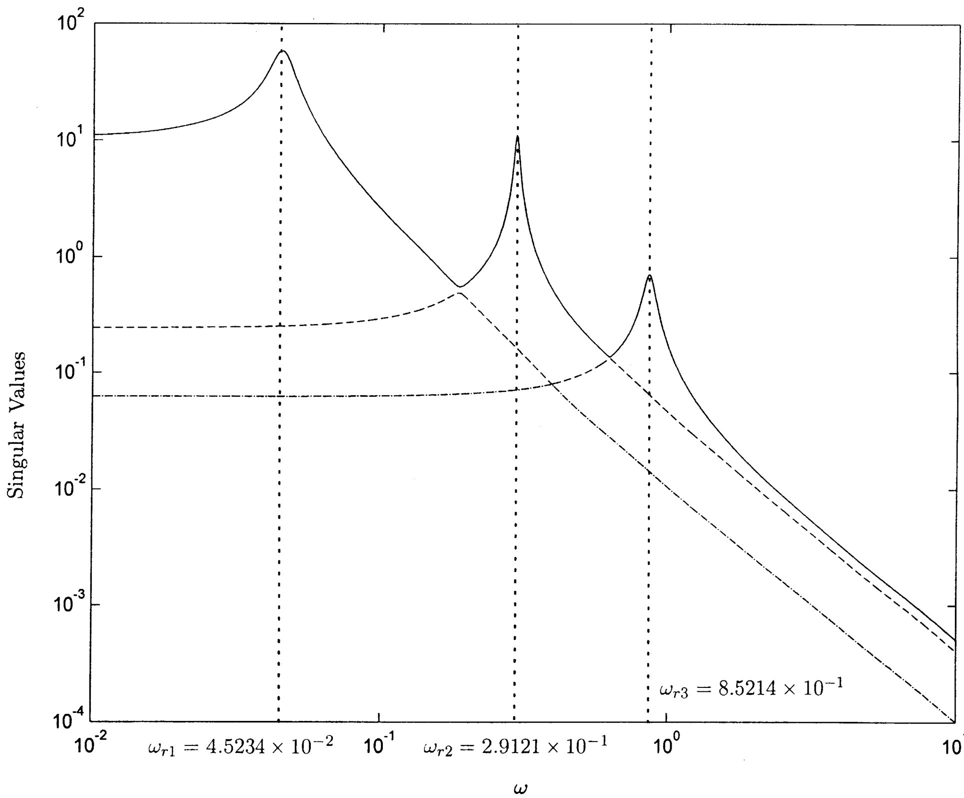

Figure 12. Singular values of the mass–dashpot–spring system as a function of ω (—— σ_1; - - - - - - σ_2; —·—σ_3).

instance, it can be observed in Figure 14 that components of $\mathbf{u}_2$ change abruptly when singular value loci veering for σ_2 occurs at $\omega = 0{\cdot}1825$, $0{\cdot}3872$ and $0{\cdot}6151$ rad/s. If the system is excited in the direction of the second right singular vector $\mathbf{v}_2 = \mathbf{u}_2$ and the excitation frequency ω changes from 0·1 to 0·4 rad/s, the input–output relationships will change significantly; subsequently, distribution of an input between different output channels will change dramatically, which is due to inhibition of vibration propagation and consequently localization of vibration modes as a function of excitation frequency ω. Meanwhile, singular values change smoothly that means power and energy transmission ratios are smooth. The only abrupt change in singular values (and subsequently in power and energy transmission ratios) occurs at resonance frequencies.

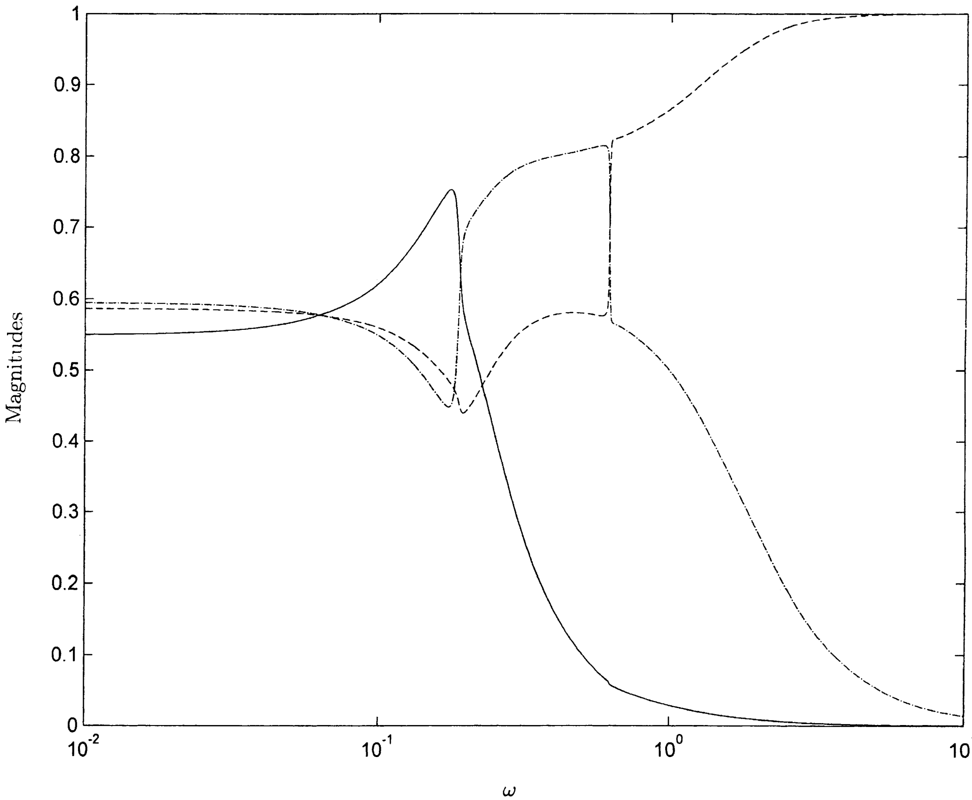

Figure 13. Magnitudes of the left singular vector $\mathbf{u}_1$ as a function of ω (—— $|u_{1,1}|$; - - - - - - $|u_{1,2}|$; —·— $|u_{1,3}|$).

In order to detect the onset of localization in input–output relationships, the matrix transfer function of this system is studied as well. Unlike the eigenvalues and eigenvectors, effects of the disorder on matrix transfer function components $G_{ij}(s)$ are smooth for both weakly and strongly coupled systems in numerical examples, not presented here for limited space. The characteristics of $G_{ij}(s)$, which quantify the effect of the input acting at the jth degree of freedom on the ith degree of freedom, are similar to those of the singular values; in particular, the largest singular value σ_1.

6. CONCLUSIONS

In this paper, input–output relationships of structures are studied by using the SVD with an emphasis to localization and curve veering phenomena. The SVD-based analysis is well suited to study the directional properties of inputs and outputs of a system. If an input is distributed in the direction of a right singular vector $\mathbf{v}_i$, the system response will be distributed to the system degrees of freedom in the direction of associated left singular vector $\mathbf{u}_i$ with a gain that is equal to the corresponding singular value σ_i. In an extent to mode localization and eigenvalue loci veering phenomena of weakly coupled disordered systems, existence of singular vector localization and singular value loci veering phenomena (occurring at the so-called isopower frequencies) are shown in weakly and

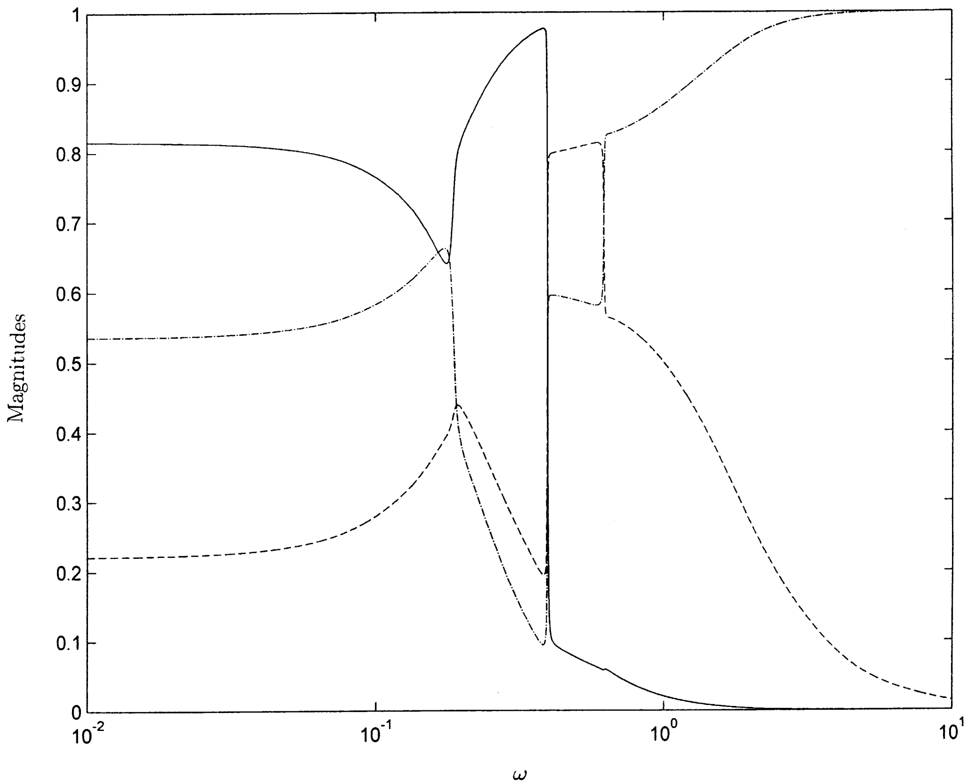

Figure 14. Magnitudes of the left singular vector $\mathbf{u}_2$ as a function of ω (—— $|u_{2,1}|$; - - - - - - $|u_{2,2}|$; —·— $|u_{2,3}|$.

strongly coupled systems. Occurrence of strong mode localization causes abrupt changes in input–output relationships of systems; however, the changes in singular values and input–output transfer function relationships are smooth; thus, power and energy transmission ratios change smoothly as well. As a result of singular-vector localization, the distribution of system's energy among different degrees of freedom changes drastically and abrupt changes in the outputs are observed in response to small changes in the input vector and the excitation frequency ω.

It is shown that the power and energy transmission ratios between the input and output vectors in a system are bounded by the squares of the maximum and minimum singular values of the system, which do not change significantly as the number of oscillators increases for tuned systems. The difference between the maximum and minimum singular values is typically very tight for nearly periodic tuned systems; as a result, the power and energy transmission ratios are not affected by placing the inputs in different right singular vector directions $\mathbf{v}_i$ but mainly determined by the excitation frequency ω for tuned systems. However, mistuned systems may have large $(\sigma_1 - \sigma_n)$ bandwidths and a small disorder in the system may result in significant changes in the bandwidth $(\sigma_1 - \sigma_n)$; i.e., implying sensitive power and energy transmission ratios. Since singular values are related to power and energy transmission ratios, they can be used to shape vibration absorbing or magnifying characteristics of a system. For instance, if we design a composite material or an absorber to absorb vibrations, then our goal should be to minimize σ_1 to minimize displacements in all load

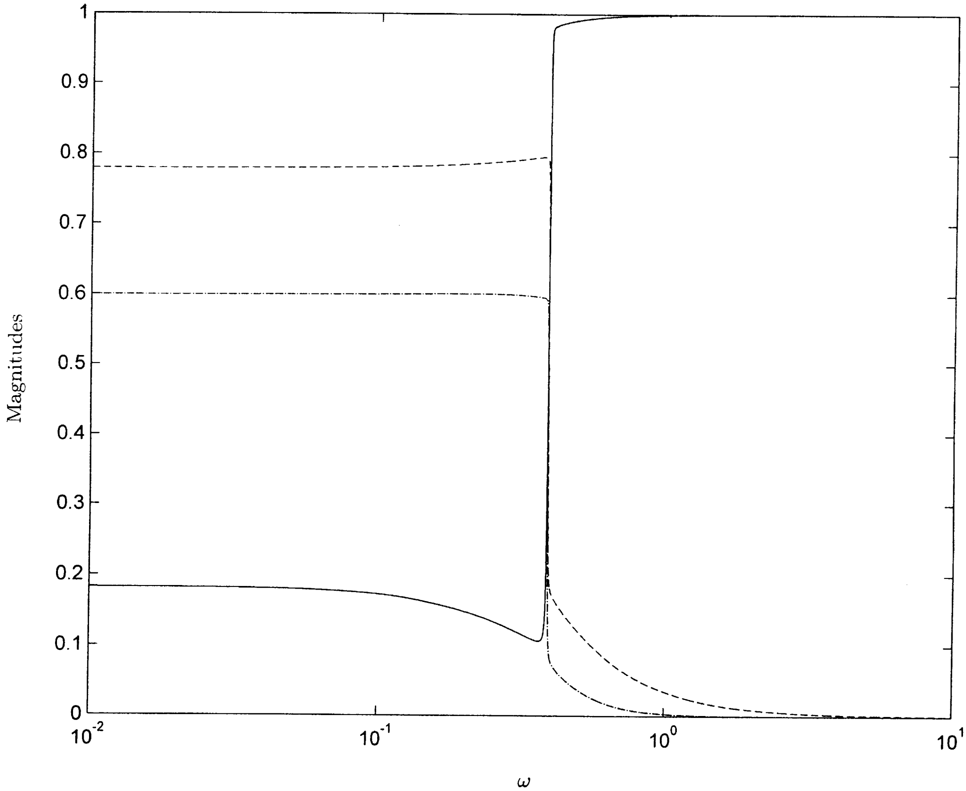

Figure 15. Magnitudes of the left singular vector $\mathbf{u}_3$ as a function of ω (—— $|u_{3,1}|$; - - - - - - $|u_{3,2}|$; —·— $|u_{3,3}|$.

cases. It is found in design trials on lumped parameter systems that using singular values in such tasks has computationally advantages over using frequency domain constraints, which has been under investigation.

If the worst forced vibration case of a structure is sought in the existence of multiple load cases, forced response for each load case should be investigated which is cumbersome; the use of singular values is computationally advantageous in this case. To this end, σ_1 has a special meaning since it is the largest system gain and corresponding right and left singular vectors $\mathbf{v}_1$ and $\mathbf{u}_1$ give, respectively, the worst possible load case and the corresponding system response. While eigenvalue-based analyses give information about the resonance frequencies and vibration modes of a structure, singular values of the structure are related to the forced response characteristics and give the dynamic behavior in the frequency domain.

ACKNOWLEDGMENTS

This research was supported in part by Istanbul Technical University Research Foundation. The author would like to thank Prof. Noboru Kikuchi and Assoc. Prof. Gregory M. Hulbert of the University of Michigan and the anonymous reviewer for helpful suggestions and corrections.

REFERENCES

1. P. W. Anderson 1958 *Physical Review* **109**, 1492–1505. Absence of diffusion in certain random lattices.
2. A. Golshani, H. Pier, E. Kapon and M. Moser 1999 *Journal of Applied Physics* **85**, 2454–2457. Photon mode localization in disordered arrays of vertical cavity surface emitting lasers.
3. K. Ishii 1973 *Supplement of the Progress of Theoretical Physics* **53**, 77–138. Localization of eigenvalues and transport phenomena in the one- dimensional disordered system.
4. E. W. Montroll and R. B. Potts 1955 *Physical Review* **100**, 525–543. Effect of defects on lattice vibration.
5. H. B. Rosenstock and R. E. McGill 1962 *Journal of Mathematical Physics* **3**, 200–202. Vibrational modes of disordered linear chains.
6. O. O. Bendiksen 1984 *Proceedings of the XVIth International Congress of Theoretical and Applied Mechanics, Lyngby, Denmark*, 19–25. Aeroelastic stabilization by disorder and imperfections.
7. C. W. Cai, Y. K. Cheung and H. C. Chan 1995 *Journal of Applied Mechanics* **62**, 141–149. Mode localization phenomena in nearly periodic systems.
8. J. H. Ginsberg and H. Pham 1995 *Journal of Vibration and Acoustics* **117**, 439–445. Forced harmonic response of a continuous system displaying eigenvalue veering phenomena.
9. C. H. Hodges 1982 *Journal of Sound and Vibration* **82**, 441–424. Confinement of vibration by structural irregularity.
10. R. A. Ibrahim 1987 *Applied Mechanics Reviews* **40**, 309–328. Structural dynamics with parameter uncertainties.
11. C. Pierre, 1988 *Journal of Sound and Vibration* **126**, 485–502. Mode localization and eigenvalue loci veering phenomena in disordered structures.
12. C. Pierre and E. H. Dowell 1987 *Journal of Sound and Vibration* **114**, 549-564. Localization of Vibrations by Structural Irregularity.
13. C. Pierre, D. M. Tang and E. H. Dowell 1987 *American Institute of Aeronautics and Astronautics Journal* **25**, 1249–1257. Localized vibrations of disordered multi-span beams: theory and experiment.
14. N. A. Valero and O. O. Bendiksen 1986 *American Society of Mechanical Engineers Journal of Engineering for Gas Turbines and Power* **108**, 293–299. Vibration characteristics of mistuned shrouded blade assemblies.
15. A. W. Leissa 1974 *Journal of Applied Mathematics and Physics (ZAMP)* **25**, 99–111. On a curve veering aberration.
16. N. C. Perkins and C. D. Mote Jr. 1986 *Journal of Sound and Vibration* **106**, 451–463. Comments on curve veering in eigenvalue problems.
17. V. C. Klema and A. J. Laub 1980 *IEEE Transactions on Automatic Control* **25**, 164–176. The singular value decomposition: its computation and some applications.
18. W. H. Press, S. A. Teukolsky, W. T. Vetterling and B.P. Flannery 1992 *Numerical Recipes*. Cambridge, England; Cambridge University Press.
19. J. S. Freudenberg and D. P. Looze 1988 *Frequency Domain Properties of Scalar and Multivariable Feedback Systems*. Berlin: Springer-Verlag.
20. G. H. Golub and C. F. Van Loan 1983 *Matrix Computations*. Baltimore: Johns Hopkins University Press.
21. A. G. J. MacFarlane and D. F. A. Scott-Jones 1979 *International Journal of Control* **29**, 65–91. Vector gain.
22. I. Postlethwaite, J. M. Edmunds and A. G. J. MacFarlane 1981 *IEEE Transactions on Automatic Control* **AC-26**, 32–46. Principal gains and principle phases in the analysis of linear multivariable feedback systems.
23. R. A. Horn and C. R. Johnson 1991 *Topics in Matrix Analysis*. Cambridge: Cambridge University Press.